LANGMUIR

pubs.acs.org/Langmuir Article

Interfacial Features Govern Nanoscale Jumping Droplets

Kimia Montazeri, Penghui Cao, and Yoonjin Won*

Cite This: *Langmuir* 2023, 39, 4317−4325 Read Online

ACCESS | Metrics & More | Article Recommendations

ABSTRACT: The solid surfaces with different profile levels impact the liquid−solid contact nature and hence wetting characteristics, showing a vital role in liquid droplets' mobility and dynamic behaviors. Therefore, engineering nanostructured features ultimately enables tuning and controlling the dynamic motion of droplets. In this study, we demonstrate an approach to manipulate nanodroplets' motion behaviors in contact with a surface through tailoring the surface morphological profile. By tracking the trajectories of water molecules at the interface, we find that the motions of a nanodroplet subjected to different levels of lateral force reveal various modes that are identified as *creeping*, *rolling*, and *jumping* motions. Interestingly, the elastic deformation of the droplet and sudden changes in the receding contact angle provide the mechanistic origin for droplet jumping. Guided by computational simulations, a regime map delineating the droplet motion modes with surface profile levels and applied forces is constructed, providing a design strategy for controlling droplet motions via surface engineering.

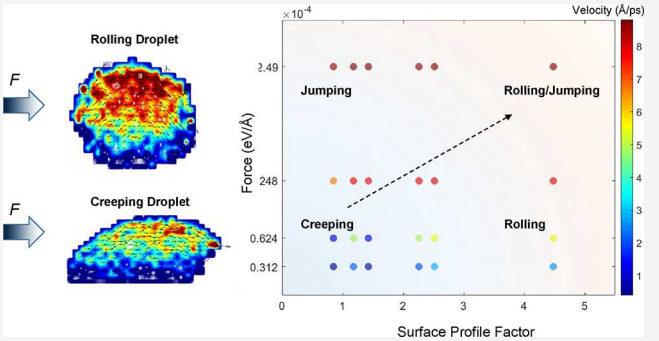

INTRODUCTION

Nanoscale interfacial phenomena are ubiquitous, and their behavior plays an important role in manipulating interfacial and phase change performnaces. The examples utilizing interfacial phenomena in nature (Figure 1a,b) include plant leaves (e.g., lotus) that enable self-cleaning and anti-icing performances through their hydrophobic characteristics.[1,2] Among multiple interfacial phenomena, engineering droplet dynamics can benefit broad applications,[3] such as phase change surfaces (by facilliating dropwise condensation),[4,5] water-repellent surfaces[6] (that can be used for water harvesting and collection), and the design of batteries or electrolytes. Utilizing nano- or micropatterns (e.g., grooves[5] and pillars[7]) on surfaces is known to transform their solid−liquid contact behavior by enabling superhydrophobicity.[8,9] Surface roughness can be modified across a wide range[10] by fabricating microscale and nanoscale structures with various shapes[11] such as sintered particles,[12] pillars and grooves,[5,7,13,14] meshes,[15,16] and nanowires.[17] In addition to this, the thicknesses and length scales of such structures can range from a few angstroms to several nano[18] or micrometers.[19]

There have been several studies in the literature dedicated to the investigation of surface interactions with water from a molecular perspective, such as the wettability of flat surfaces of carbon nanotubes,[24] crystalline polyethylene surfaces,[25] quartz surfaces,[26] and graphene-coated surfaces.[27] However, the majority of previous studies has investigated the effects of the geometrical attributes and chemistry of surfaces on the equilibrium or static state of droplets.[20] Examples of previous studies focused on the effects of pillar heights and interfacial area on wetting states[21,22] or external fields (e.g., electric field[23] or external body forces[14]).

Although the effects of surface structures on their wetting characteristics have been extensively studied, it is still unclear how these surface structures can alter droplet dynamics on such surfaces,[28] which is necessary for engineering moving droplets. In addition, it has been nearly impossible to experimentally capture nanodroplets and their dynamic motions near the contact area with solid. The dynamic interfacial contact line between solid and liquid surfaces is affected by the molecular-scale structures;[29] therefore, most of the available models lack the accuracy required for dealing with molecular interactions in surfaces with nanoscale roughnesses.[30−32] A proper understanding of the dominant mechanisms of droplet motion on rough surfaces is essential for efficient control of droplet motion and tailoring of their dynamics for specific applications.[33]

In this study, we investigate the combined effect of morphological characteristics and external body forces on

Received: December 7, 2022
Revised: February 14, 2023
Published: March 16, 2023

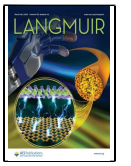

https://doi.org/10.1021/acs.langmuir.2c03313
Langmuir 2023, 39, 4317−4325

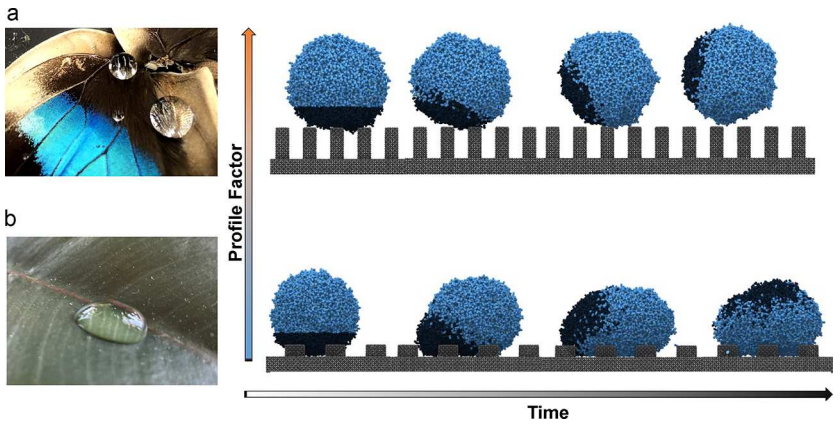

Figure 1. Dynamic motion behaviors of water droplets on rough surfaces. The images show water droplets on a (a) butterfly wing and (b) a leaf. The nanostructured textures of the butterfly wing enable superhydrophobic wettability. Our simulations illustrate how nanodroplets behave on surfaces with different profile factors, as represented in time-lapse snapshots. A nanodroplet on the surface with a high profile factor has a smaller contact area and maintains its spherical shape with minimum deformation when subjected to external forces, leading to rolling−jumping motions. A droplet on a surface with a low profile factor results in the deformation of the droplet shape and creeping motion. The surfaces observed from nature motivate us to mimic these profiles to control the droplet dynamics.

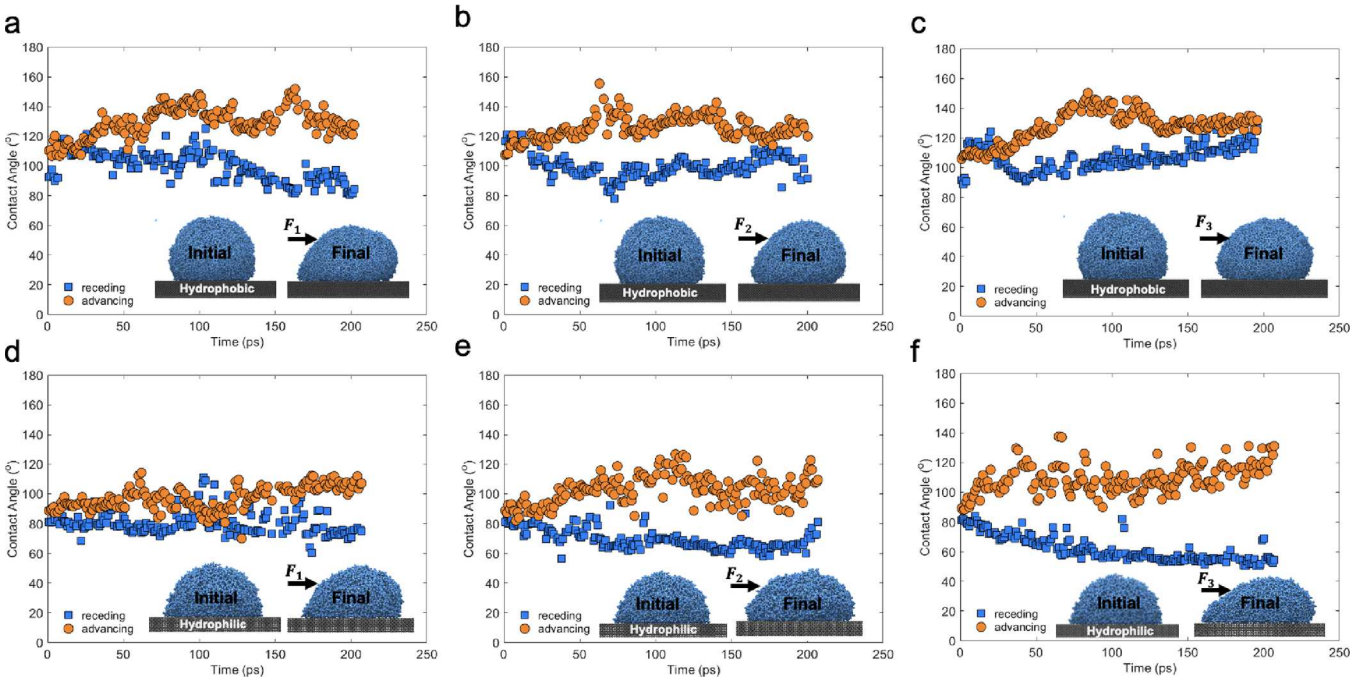

Figure 2. Dynamic contact angle of a droplet on hydrophobic and hydrophilic surfaces. (a−c) Plots showing the effects of force on the dynamic advancing (circle) and receding (square) contact angles of a nanodroplet on a flat hydrophobic surface (where the van der Waals energy between solid and liquid atoms is 0.0073 eV). As the value of force increases from F1 = 3.12×10^{-5} eV/Å to F3 = 1.24×10^{-4} eV/Å, the difference between the advancing and receding contact angle (that is contact angle hysteresis) decreases. (d−f) Plots showing the effects of force on the dynamic advancing and receding contact angle of a droplet on a flat hydrophilic surface (where the van der Waals energy between solid and liquid atoms is 0.0111 eV). In contrast to the hydrophobic surface, the contact angle hysteresis increases as the force increases on a hydrophilic surface, evidencing a crawling motion.

droplet dynamics from a nanoscale perspective by employing molecular dynamics simulations. Moving droplets are simulated on surfaces with different surface profile factors. Their motions are identified as *creeping*, *rolling*, or *jumping* depending on the combination of the location and velocity of water molecules in a droplet, the droplet rotations, and the evolution in liquid−vapor−solid contact lines (Figure 1). This allows us to gain a deeper understanding of the change in droplet motion modes due to surface engineering, which is critical to elucidate the physics behind droplet dynamics and to design surfaces with desired characteristics. The knowledge can be used to develop a regime map and guidelines for the design of efficient water collecting surfaces where the control of nanosized water droplets is essential.

RESULTS

Droplets on Flat Surfaces. We first investigate the evolution of the droplet on a flat surface with either hydrophobic or hydrophilic characteristics (with van der Waals energies of 0.0073 and 0.0111 eV, corresponding to

https://doi.org/10.1021/acs.langmuir.2c03313
Langmuir 2023, 39, 4317−4325

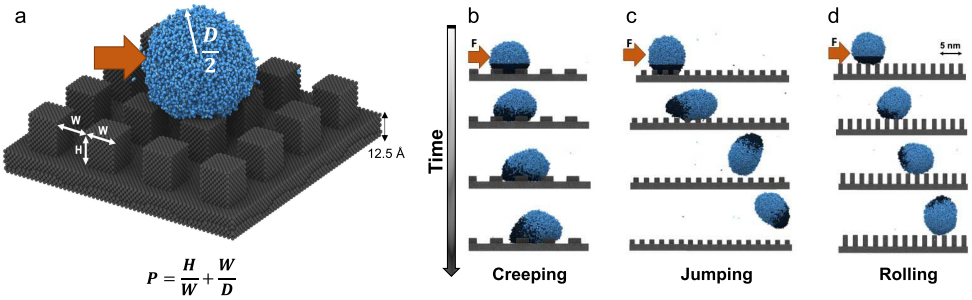

Figure 3. Droplet motion modes. (a) Surface profile factor P is defined based on the geometrical parameters of the grooves, such as width (W), channel size (W; same with the width), and height (H), as well as a droplet diameter (D). Time-lapse images of droplets are shown from molecular dynamics simulations where the initial molecules that contact with a solid surface are shown in dark colors in (b–d). (b) Time-lapse captures show the creeping motion of a droplet where there is a significant velocity gradient between the interfacial water molecules and the surface molecules. The large gradient results in the deformation of the droplet and its creeping motion. (c) Captures show the jumping motion of a droplet. Jumping occurs when the body force overcomes the interaction forces between the liquid and solid molecules and causes the droplet to deattach from the surface. (d) Captures show the rolling motion of a droplet. In the rolling motion mode, the surface and interfacial molecules constantly change their locations, while the center of mass of the droplet only moves in the direction of the force.

the static contact angles of 120 and 87°, respectively; see the Methods section for the details). Once an external force is applied to all the molecules, we calculate the dynamic contact angles (e.g., advancing and receding contact angles representing the contact angles of leading and receding edges of the droplet, respectively). Here, the applied external force represents various potential boundary conditions, such as the gravitational force for a droplet on a tilted surface,[34] vapor expansion forces during boiling phenomena,[35,36] electrostatic forces (e.g., charged droplets can react to electrostatic forces),[37] magnetic forces (e.g., droplets containing metallic particles can react to magnetic forces), van der Waals forces between adjacent droplets, and attractive forces between a single droplet and the surface.[38] For example, when a droplet sits on a tilted surface, it deforms with the presence of the gravitational force. Before the droplet starts moving, this gravitational force is in balance with the adhesion force between the droplet and the rough surface. However, increasing the inclination angle of the surface results in an increase in the gravitational body force, which further results in a decrease in the receding contact angle and an increase in the advancing contact angle.

To identify the combined impact of surface wettability and external force on droplet dynamics, the dynamic contact angles of a nanodroplet with a diameter of 60 Å, consisting of 8000 water molecules on a flat surface, are obtained and presented in Figure 2. Figure 2a–c shows the dynamic advancing and receding contact angles of a nanodroplet on a hydrophobic surface, where the van der Waals energy between solid and liquid atoms is 0.0073 eV (static contact angle = 120°). Figure 2d–f shows a nanodroplet on a hydrophilic surface with the van der Waals energy of 0.0111 eV (static contact angle = 87°). For small external forces (F1 = 3.12×10^{-5} eV/Å) in Figure 2a, the droplet tends to slightly deform with an increase in the advancing contact angle and a consequent decrease in the receding contact angle. Therefore, as the droplet moves on the flat surface, the contact angle hysteresis, which is defined as the difference between advancing and receding contact angles, increases. Inversely, for larger forces (F3 = 1.24×10^{-4} eV/Å) in Figure 2c, the contact area between the droplet and the surface becomes smaller as the droplet regains its spherical shape; hence, the contact angle hysteresis decreases. On hydrophilic surfaces (Figure 2d–f), increasing the external force from F1 to F3 results in more deformation of the nanodroplet and an increase in the contact angle hysteresis. Our results suggest that the combination of surface wettability and external force allows droplets to move on flat surfaces; however, any significant variations of the droplet motion mode are not observed. The droplets on a flat surface mostly creep, crawl, or slide instead of showing any dynamic phenomena like jumping.

DESIGN OF NANOPROFILE

In real-life applications, surfaces are rarely smooth, and most surfaces show a certain level of surface profile or roughness. For example, Figure 1a shows that surfaces from nature, such as butterfly wings and plant leaves, show different droplet dynamics due to their inherent natural roughness attributed to their micro- and nanoscale structures. Butterfly wings are known as self-cleaning surfaces due to their capability to make droplets always roll and keep the wings dry. Therefore, there have been significant efforts to understand and mimic the architectures of butterfly wings, but the understanding of the roughness's impact on the dynamic droplet behavior at the nanoscale is still lacking. To address this challenge, we cover a wide range of surface roughnesses by systematically manipulating the surface parameters and investigate their impact on droplet dynamics with hydrophobic characteristics (with a static contact angle of >100°).

Here, the surface profile factor is defined by using geometrical parameters, including the aspect ratio of grooves (H/W) and the nondimensional characteristic length of a droplet (W/D): $P = \frac{H}{W} + \frac{W}{D}$, where H and W are the height and width of a groove, respectively, and D is the diameter of a water droplet (see Figure 3a). The profile factor in this study ranges from P1 = 0.85 to P6 = 4.47, representing various types of geometrical attributes for nanostructured surfaces, which are summarized in Table 1. Figure 3a illustrates the profile factor in a simulation cell (see the Methods section for the details of the MD models).

Dynamic Motion Modes of Nanodroplets on Roughened Surfaces. Geometrical attributes of the surface and consequently the surface profile factors, as well as the level of external forces can induce various dynamic behaviors of droplets. During droplet motion on a rough surface, there is a competition between the external force and lateral friction forces. As a result of this competition between different forces,

https://doi.org/10.1021/acs.langmuir.2c03313
Langmuir 2023, 39, 4317–4325

Table 1. Geometrical Attributes and Corresponding Profile Factor for Nanostructured Surfaces

	P1	P2	P3	P4	P5	P6
height (Å)	10.84	25.30	10.84	50.61	25.30	50.61
width (Å)	25.30	25.30	10.84	25.30	10.84	10.84
profile factor	0.85	1.18	1.42	2.26	2.51	4.47

various droplet behaviors are categorized into three motions: creeping, rolling, and jumping (Figure 3). To identify different motion modes in simulations, we quantify dyanmic features such as angular velocity, center of mass velocity, and dynamic contact angles. To compute the angular or linear velocities, the water molecules that initially are contacted with the solid interface are separately marked. Further, the location of these molecules is tracked with respect to the center of mass of the droplet as the droplet moves along the surface.

Creeping. Creeping occurs when the motion of the molecules at the interface is suppressed due to strong interactions between the solid and liquid molecules, while the molecules at the interface of the droplet are less impacted by strong adhesions and have more freedom to move. Instead, the marked molecules spread near the liquid−vapor interface region as the droplet moves on the surface. The difference in movements leads to significant velocity gradients along the vertical direction and makes the water droplet deform and further spread on the surface, called the creeping motion mode (Figures 3b and 4a). In this mode, the difference between the receding and advancing contact angles increases with time as the receding angle continuously decreases.

Rolling. Water molecules on hydrophobic surfaces in many cases often rotate around the center of mass of the droplet as it advances on the rough surface, called the rolling motion mode. Due to this continuous exchange of molecules from the interface to the surface of the droplet, droplets roll on the surface while maintaining their spherical shapes (Figures 3d and 4b,c). In this case, the center of mass of the droplet moves with a velocity that corresponds to the applied body force in the motion direction. The constant rotation of surface molecules around the center of mass of the droplet can be observed in Figure 4b,c. The different colors within droplets help us quantify droplet rotation by calculating droplet angular velocities.

Jumping. Jumping is a motion mode that typically follows the rolling motion and occurs when the interaction forces between the liquid droplet and the surface are much smaller than the interatomic interactions between liquid particles (Figure 3c). The applied force on the droplet overcomes the attractive forces between the liquid droplet and solid surface, resulting in the separation of the droplet from the surface. This mode occurs mostly with high external forces regardless of the surface profile factors. A jumping mode is indicated by a sudden increase in the value of the receding contact angle or height. This occurs since the contact area of the droplet with the surface rapidly decreases as the droplet gradually regains its spherical shape. The asymmetric shape of the droplet with a small contact area with the surface creates a favorable condition for the droplet to deattach from the surface.

Effects of Profile Factor on Motion Modes. The surface profile factor is one of the most contributing parameters to droplet dynamic behaviors if the external force is relatively small. A series of snapshots with a time interval of 50 ps of the droplet motion on different heights and associated profile factors are shown in Figure 4, in which the droplets are subjected to the same force of F1 = 3.12×10^{-5} eV/Å. As the groove height increases from 10.84 to 50.61 Å and the groove widths decreases from 25.30 to 10.84 Å (i.e., surface profile factor increases from P1 = 0.85 to P6 = 4.47 from Figure 4a−c), the motion exhibits a transition from creeping to rolling motion mode. Correspondingly, the steady-state linear velocity of the droplet increases from 1 to ∼9 Å/ps where its angular velocity increases up to 0.01 π/ps, as the color gradient within droplets indicates.

Effects of Force on Motion Modes. The level of external force dominates the droplet dynamic behaviors for the surfaces with smaller profile factors. Therefore, we separately

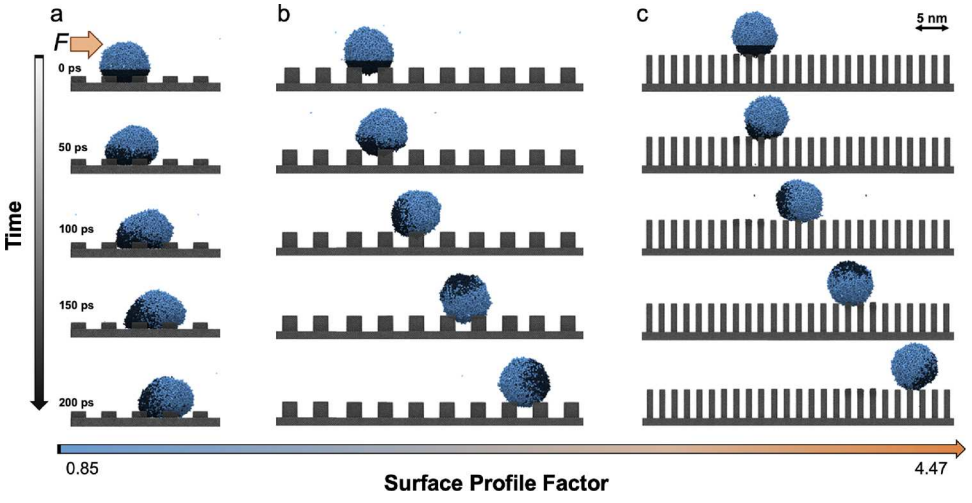

Figure 4. Effects of the surface profile factor on droplet motion. (a−c) Snapshot time series show the droplet motion mode for profile factor in the range of P1 = 0.85 to P6 = 4.47, subject to an external force equal to F1 = 3.12×10^{-5} eV/Å. For a small force (F1), the surface profile factor plays a key role in determining the most dominant factor in droplet motions. For surfaces with a low profile factor (with a small groove height of 10.84 Å; P1 = 0.85), the droplet tends to deform with a large contact area with the solid surface and moves in the creeping motion mode. The same small force causes a droplet on a rough surface (with a groove height of 50.61 Å; P6 = 4.47) to move with the rolling motion mode. The water molecules near the solid surface are marked with dark blue color to locate their positions and angular velocities in later stages of the simulation.

https://doi.org/10.1021/acs.langmuir.2c03313
Langmuir 2023, 39, 4317−4325

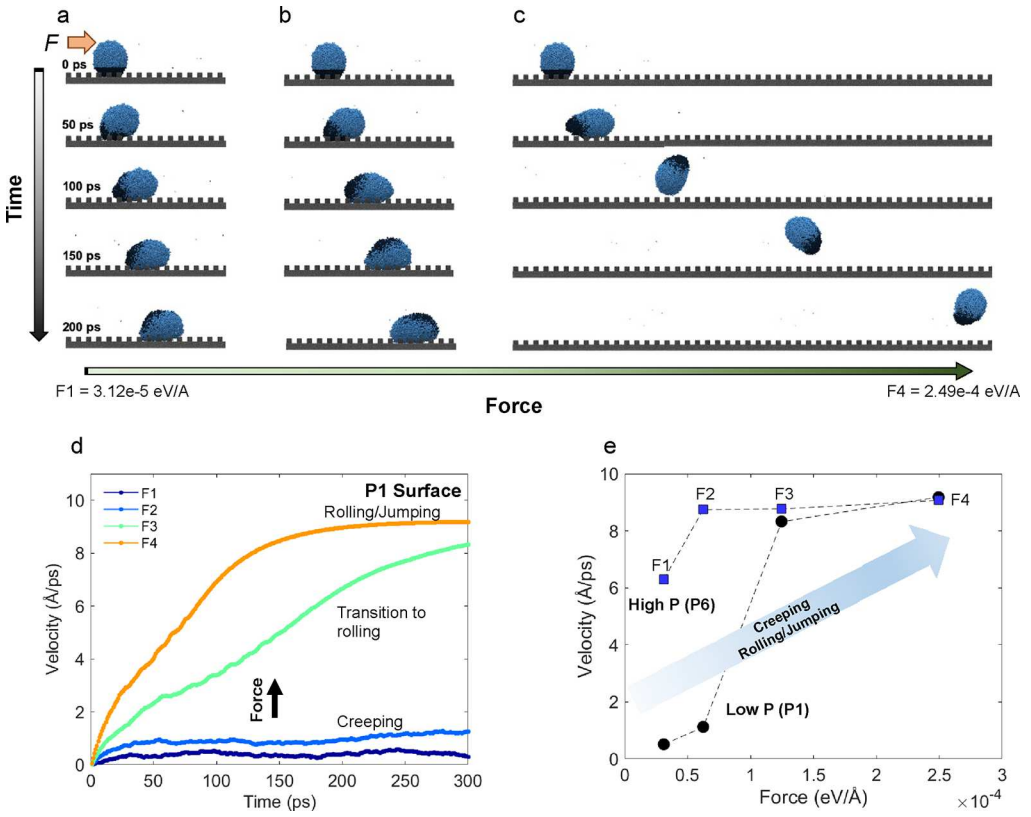

Figure 5. Dynamic motion of the droplet as a result of applied force. (a–c) Time-lapse images of droplets on a rough surface (P3) for different external forces (F1, F2, and F4). As the force increases from F1 to F4, the motion modes change from the creeping to rolling and eventually jumping motion. (d) Plot showing the velocity of the center of mass of the droplet for different forces applied (P1 surface), describing two different mechanisms: for small forces (F1 and F2), the velocity of the center remains almost constant with time due to droplet deformation and creeping motion mode. For large forces (F3 and F4), the steady-state velocity increases and then converges to a constant value, where the dominant motion mode of the droplet is rolling and jumping. (e) Plot showing the steady-state velocity of the droplet for two different surface profile factors of P1 (circle) and P6 (square). The creeping motion mode at small forces changes to rolling and jumping for larger forces.

investigate dynamic droplet motion modes by varying the applied force from F1 = 3.12×10^{-5} to F4 = 2.49×10^{-4} eV/Å with a surface profile factor of P3 = 1.42. The time-lapse droplet images in Figure 5a–c show the transition from creeping motion mode for small forces to rolling and jumping for larger forces. At smaller forces (F1 or F2), the velocity of the center of mass reaches a constant value after a certain simulation time (less than 100 ps), and the droplet motion reaches steady-state motion, showing a creeping motion mode based on the velocities. in Figure 5d. At larger forces (F3 or F4), the steady-state velocity is reached at later stages of the simulation (>300 ps), where the droplet motion mode is considered as the rolling–jumping. The effect of force on the droplet mobility is summarized in Figure 5e, where the transition between the creeping motion mode and rolling and jumping is emphasized.

Transient Phenomena of Droplet Motions. To fully explore the transition between the droplet motion modes with varying surface profile factors and external forces, the time-dependent velocities of the center of mass of the droplet for different combinations (e.g., F1 = 3.12×10^{-5} eV/Å to F4 = 2.49×10^{-4} eV/Å and P1 = 0.85 to P6 = 4.47) are recorded. Here, for smaller forces (F1) in Figure 6a, the surface profile factor is dominant to determine the modes of motion. As forces increase from Figure 6b to 6d (compared to Figure 6a), the transitions from creeping to rolling and jumping are observed. In general, as the profile factor and force increase, the steady-state velocity tends to converge to a constant and equal value; however, the sharp transition between the creeping and rolling motion mode occurs for a surface with the largest groove height (where the groove height is 63.2 Å; P3 = 1.42). In summary, the droplet motion mode changes from the creeping motion mode to rolling and eventually jumping from the surface with either a larger profile factor or an external force.

Combined Effects of Profile Factor and Force toward Design Guidelines. The dynamic contact angles of droplets and corresponding motion modes are reported in Figure 7a. The various behaviors in the shape of the droplet, as it moves on the surface, result in different trends in the dynamic contact angles, which can serve as indicators for the droplet motion behavior. For instance, on surfaces with a low profile factor (i.e., P1, P2, and P3) and force F1, droplets deform significantly, resulting in a continuous drop in the receding angle while the advancing contact angle increases (Figure 7a). This diverging trend in the contact angle hysteresis is an indicator of the creeping motion mode. In contrast, on surfaces with a low profile factor and large forces, initially, the droplet experiences large elastic deformations; however, eventually, the external force overcomes the adhesion forces, which results in a sudden increase in the receding angle. This sudden increase indicates the jumping motion mode due to the decreasing contact area of the droplet with the surface and results in an asymmetric and deformed droplet.

https://doi.org/10.1021/acs.langmuir.2c03313
Langmuir 2023, 39, 4317–4325

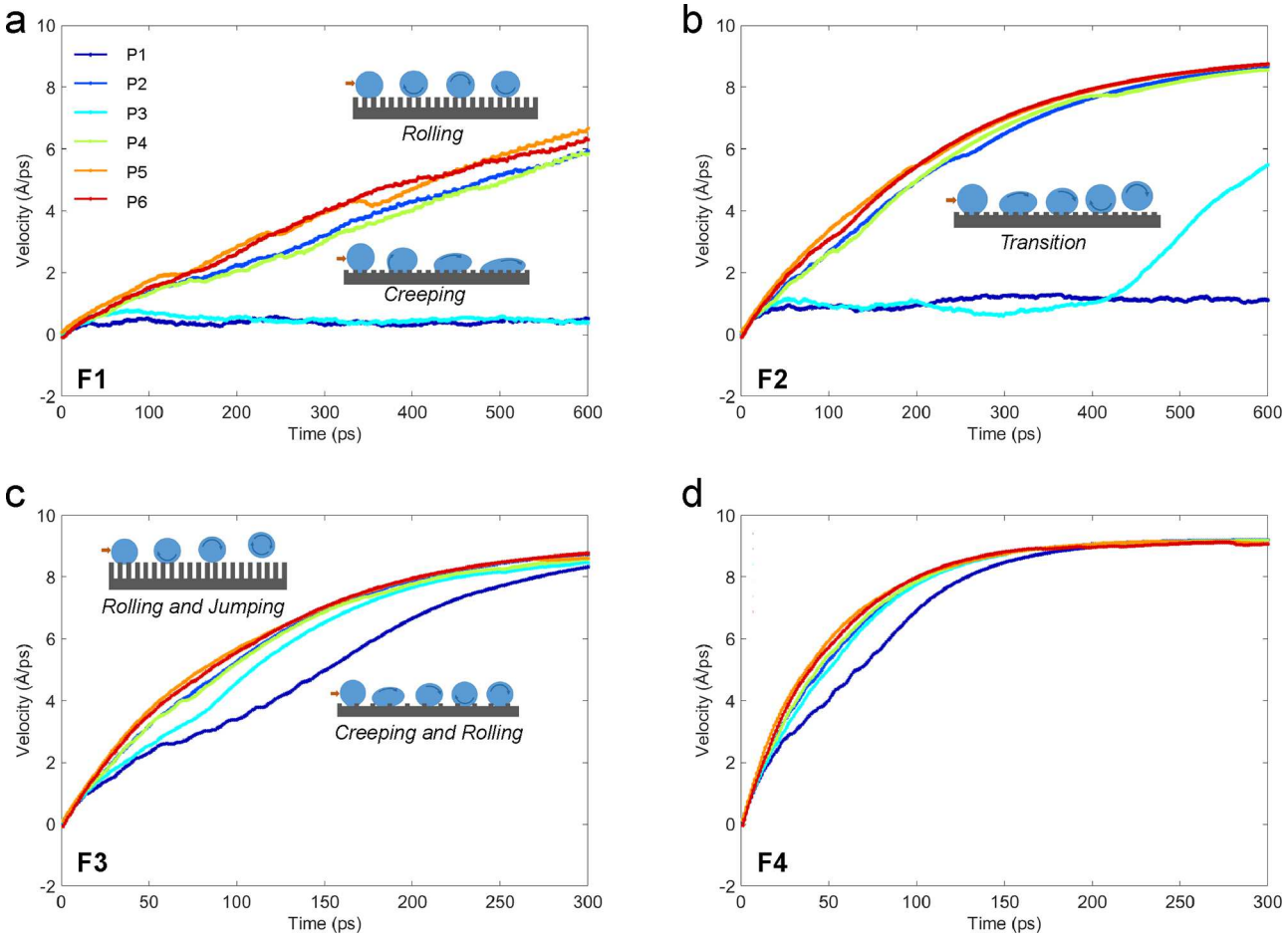

Figure 6. Transition behaviors of droplet mobility with varying profile factors and forces. Plots showing the transient velocity of droplets for different profile factors in the range of P1 to P6 with an external force of F1 to F4 (a–d). (a, b) For smaller forces, there is a significant difference between the modes of motion on surfaces with different profile factors. For surfaces with a low profile factor, in particular, with small groove heights, a droplet tends to deform showing a creeping motion mode. The same small force causes droplets with a high profile factor to move with a rolling motion mode. (c, d) As the forces increase to F3 and F4, the dominant mode of motion becomes rolling and jumping. The difference between the surface profiles becomes less significant.

The understanding of the combined effects of these two parameters on droplet motions is essential for controlling the mobility of water nanodroplets subject to external forces on rough surfaces. Considering the combined effects of surface profile factor and external body force, we have categorized the motion modes of the droplet into four distinct regions in a regime map in Figure 7b by quantifying the dynamic characteristics of droplets. The regime map is a valuable measure that can aid researchers in developing a design strategy for tuning and controlling droplet motion via surface engineering.

DISCUSSION AND CONCLUSIONS

The goal of this paper is to explore a previously undefined regime using molecular dynamics models. In this study, dynamic characteristics of moving droplets, such as dynamic wetting, molecule positions, and velocities, are directly computed from molecular dynamics simulations, which can not be obtained from either continuum scale models or by experimental methods.[39] Molecular dynamics models allow the understanding of how nanodroplets can physically behave differently from larger droplets,[40−45] which have not been observed through experiments. The simulation models are developed and performed carefully (by using suitable force fields and models such as TIP4P that have proven to predict thermophysical properties of both water and solid surfaces) to investigate the fundamental and dynamic behaviors at the atomic level.

As the scale goes down, it becomes extremely challenging to maintain thermally stable nanodroplets without experiencing heat and mass transfer across their liquid−vapor interfaces. Therefore, the next level goal of this study is to further understand the dynamic motion of nanodroplets on roughned surfaces, subjected to external forces. Different combinations of morphological parameters, surface wettability, and external forces have been tested that lead to various modes of droplet motions. Three different motion modes such as creeping, rolling, and jumping motions are identified based on linear and angular trajectory on rough surfaces, and a regime map is integrated to predict droplet motion based on different combinations of geometrical parameters and external forces. The insights provide profound implications for the design of specific surfaces for certain applications, for instance, the engineered jumping motion of the droplet toward self-cleaning[46] and anti-icing[47] and anti-frosting[48] properties.

https://doi.org/10.1021/acs.langmuir.2c03313
Langmuir 2023, 39, 4317−4325

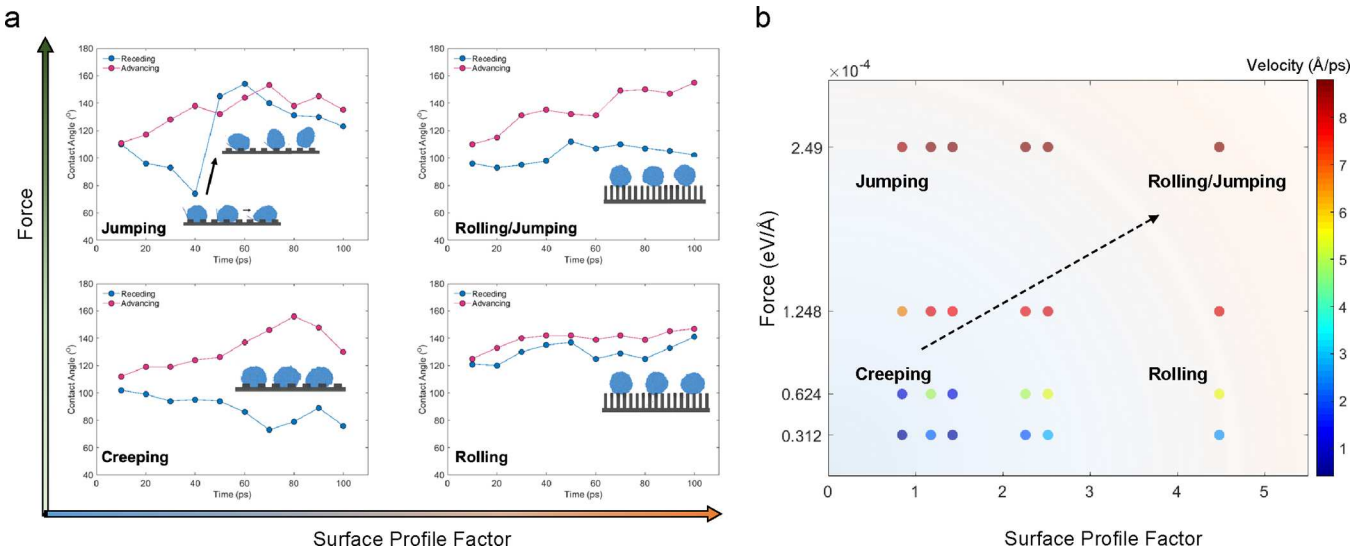

Figure 7. Regime map showing droplet motion modes. (a) Plots showing the dynamic advancing and receding contact angles as a result of the surface profile factor and the external force applied. (b) The nanodroplet velocities are used to create a regime map, showing the droplet velocity ranges. The values of velocity magnitude are indicated with different colors, identifying different modes of droplet motion ranging from creeping, rolling, and jumping. For surfaces with low profile factor values (i.e., P1, P2, and P3) and small forces (i.e., F1 and F2), droplets tend to creep on the surface with large shape deformation. As the profile factor increases (P4, P5, and P6), the motion changes toward rolling.

METHODS

The goal of this study is to explore previous undefined regime by taking advantages of using MD models. The MD models allow us to explore how nanodroplets can physically behave differently, which have not been observed through experiments. MD simulations are performed using LAMMPS (large scale atomic/molecular massively parallel simulator).[49] A water droplet consisting of 8000 water molecules is placed on nanostructured surfaces with different heights and widths to account for various surface profile factor. Solid atoms are arranged in a face-centered cubic (FCC) structure with a lattice parameter of 3.615 Å. The solid−solid interactions are not considered in this study and solid atoms only interact with the liquid molecules. The solid atoms are excluded from time integration and therefore are fixed through all the simulations.

Water molecules are modeled by the TIP4P-Ew water model,[50] which is a four-site water model and allocates two sites from hydrogen, one site for oxygen and one site for the negative charge of the oxygen atom along the bisector of the H−O−H angle. The SHAKE algorithm is used to keep the O−H and H−H bonds and the H−O−H angle rigid. This model represents atomistic behaviors of water molecules and predicts their thermophysical properties. To describe the interactions between the solid atoms and the oxygen atoms and oxygen−oxygen interactions, Lennard Jones (LJ) potential is used with a cutoff distance of 12 Å and σ = 2.75185 Å. The depth of the potential well ϵ is changed from 0.00737 to 0.0111 eV to represent hydrophobic and hydrophilic flat surfaces, respectively. Long-range coulombic interactions are calculated by using a particle−particle−particle−mesh (PPPM) solver.[51]

Nanostructures are created as rectangular grooves on a solid slab with a thickness of 12.56 Å. To account for various surface profile factors, we consider different groove heights, groove widths, and channel sizes. Six profile factors are considered in this study, ranging from P1 = 0.85 to P6 = 4.47. The surface profile factor is a unitless parameter, defined with two terms based on the aspect ratio of the grooves and the nondimensional characteristic length of the droplet, which is defined as the diameter of the droplet divided by the groove width. In this study, for consistency, the width and the channel size between the grooves are considered to be equal and are varied between 10.84 and 25.30 Å, while three different groove heights of 10.84, 25.30, and 50.61 Å are considered. The details of the groove geometrical dimensions are shown in Table 1.

Initially, the water droplet is placed on top of the grooves in a cubic arrangement. Then, the system is relaxed in NVT ensemble (constant number of particles, constant volume, and constant temperature) at 300 K for 1 ns. After the equilibrium has been reached, the droplet obtains its relaxed shape in contact with each surface, depending on the properties of the surface, i.e., the characteristic energy between the liquid molecules and solid atoms that are defined based on LJ potentials. Periodic boundary conditions are posed in the *x*, *y*, and *z* directions to ensure particle interactions across the boundary of the system. It should be noted that the length of the system in the *x* and *y* directions is chosen such that the periodic image of the droplet does not affect the simulation results.

AUTHOR INFORMATION

Corresponding Author

Yoonjin Won − *Department of Mechanical and Aerospace Engineering and Department of Electrical Engineering and Computer Science, University of California Irvine, Irvine, California 92697, United States;* orcid.org/0000-0002-8838-6213; Email: won@uci.edu

Authors

Kimia Montazeri − *Department of Mechanical and Aerospace Engineering, University of California Irvine, Irvine, California 92697, United States*

Penghui Cao − *Department of Mechanical and Aerospace Engineering, University of California Irvine, Irvine, California 92697, United States;* orcid.org/0000-0001-9866-5075

Complete contact information is available at: https://pubs.acs.org/10.1021/acs.langmuir.2c03313

Author Contributions

Y.W. proposed and supervised the project; P.C. advised the conceptual ideas and was involved in planning and supervising. K.M. carried out the simulations, performed the computations, and analyzed the data. All authors were equally involved in writing and editing the manuscript and have given approval to the final version of the manuscript.

https://doi.org/10.1021/acs.langmuir.2c03313
Langmuir 2023, 39, 4317−4325

Notes

The authors declare no competing financial interest.

■ ACKNOWLEDGMENTS

This work was sponsored by the National Science Foundation (NSF) (grant no. CBET-TTP 1752147, Thermal Transport Processes). K.M. is thankful for the financial support from the UC Irvine Mechanical and Aerospace Engineering Department.

■ REFERENCES

(1) Neinhuis, C.; Barthlott, W. Characterization and Distribution of Water-Repellent, Self-Cleaning Plant Surfaces. *Ann. Bot.* **1997**, *79*, 667−677.
(2) Gao, X.; Jiang, L. Water-Repellent Legs of Water Striders. *Nature* **2004**, 36.
(3) Liu, X.; Liang, Y.; Zhou, F.; Liu, W. Extreme Wettability and Tunable Adhesion: Biomimicking beyond Nature? *Soft Matter* **2012**, 2070.
(4) Miljkovic, N.; Enright, R.; Wang, E. N. Effect of Droplet Morphology on Growth Dynamics and Heat Transfer during Condensation on Superhydrophobic Nanostructured Surfaces. *ACS Nano* **2012**, 1776.
(5) Xu, W.; Lan, Z.; Peng, B. L.; Wen, R. F.; Ma, X. H. Effect of Nano Structures on the Nucleus Wetting Modes during Water Vapour Condensation: From Individual Groove to Nano-Array Surface. *RSC Adv.* **2016**, *6*, 7923−7932.
(6) Zhao, C.; Montazeri, K.; Shao, B.; Won, Y. Mapping between Surface Wettability, Droplets, and Their Impacting Behaviors. *Langmuir* **2021**, 9964.
(7) Ranjan, R.; Patel, A.; Garimella, S. V.; Murthy, J. Y. Wicking and Thermal Characteristics of Micropillared Structures for Use in Passive Heat Spreaders. *Int. J. Heat Mass Transfer* **2012**, 586.
(8) Bormashenko, E.; Bormashenko, Y.; Stein, T.; Whyman, G.; Bormashenko, E. Why Do Pigeon Feathers Repel Water? Hydrophobicity of Pennae, Cassie-Baxter Wetting Hypothesis and Cassie-Wenzel Capillarity-Induced Wetting Transition. *J. Colloid Interface Sci.* **2007**, *311*, 212−216.
(9) Pandey, P. R.; Roy, S. Is It Possible to Change Wettability of Hydrophilic Surface by Changing Its Roughness? *J. Phys. Chem. Lett.* **2013**, 3692.
(10) Wang, Z.; Koratkar, N.; Ci, L.; Ajayan, P. M. Combined Micro-/Nanoscale Surface Roughness for Enhanced Hydrophobic Stability in Carbon Nanotube Arrays. *Appl. Phys. Lett.* **2007**, *90*, 143117.
(11) Koishi, T.; Yasuoka, K.; Zeng, X. C. Method to Implement Interaction Surfaces with Virtual Companion Particles for Molecular Dynamics Simulations. *J. Chem. Eng. Data* **2019**, 3693.
(12) Weibel, J. A.; Garimella, S. V.; North, M. T. Characterization of Evaporation and Boiling from Sintered Powder Wicks Fed by Capillary Action. *Int. J. Heat Mass Transfer* **2010**, 4204.
(13) Jeong, W. J.; Ha, M. Y.; Yoon, H. S.; Ambrosia, M. Dynamic Behavior of Water Droplets on Solid Surfaces with Pillar-Type Nanostructures. *Langmuir* **2012**, 5360.
(14) Li, H.; Yan, T.; Fichthorn, K. A.; Yu, S. Dynamic Contact Angles and Mechanisms of Motion of Water Droplets Moving on Nanopillared Superhydrophobic Surfaces: A Molecular Dynamics Simulation Study. *Langmuir* **2018**, 9917.
(15) Lu, G.; Yu, K.; Chen, J. Ordered Assembly of Sorted Single-Walled Carbon Nanotubes by Drying an Aqueous Droplet on a Meshed Substrate. *J. Nanosci. Nanotechnol.* **2012**, 6968.
(16) Venkateshan, D. G.; Tafreshi, H. V. Modelling Droplet Sliding Angle on Hydrophobic Wire Screens. *Colloids Surf., A* **2018**, *538*, 310−319.
(17) Seo, J.; Lee, S.; Lee, J.; Lee, T. Guided Transport of Water Droplets on Superhydrophobic-Hydrophilic Patterned Si Nanowires. *ACS Appl. Mater. Interfaces* **2011**, 4722.
(18) Cao, Q.; Cui, Z.; Shao, W. Optimization Method for Grooved Surface Structures Regarding the Evaporation Heat Transfer of Ultrathin Liquid Films at the Nanoscale. *Langmuir* **2020**, 2802.
(19) Zhang, Z.; Zhao, C. R.; Liu, M. M.; Yang, X. T. Numerical Investigation of Micrometer-Sized Droplet Impingement on Micro-Grooved Surfaces. In *International Conference on Nuclear Engineering, Proceedings, ICONE*; ICONE 2019. DOI: 10.1299/jsmeicone.2019.27.1981.
(20) Liu, G.; Fu, L.; Rode, A. V.; Craig, V. S. J. Water Droplet Motion Control on Superhydrophobic Surfaces: Exploiting the Wenzel-to-Cassie Transition. *Langmuir* **2011**, 2595.
(21) Niu, D.; Tang, G. H. Static and Dynamic Behavior of Water Droplet on Solid Surfaces with Pillar-Type Nanostructures from Molecular Dynamics Simulation. *Int. J. Heat Mass Transfer* **2014**, 647.
(22) Chen, L.; Wang, S. Y.; Xiang, X.; Tao, W. Q. Mechanism of Surface Nanostructure Changing Wettability: A Molecular Dynamics Simulation. *Comput. Mater. Sci.* **2020**, No. 109223.
(23) Daub, C. D.; Bratko, D.; Leung, K.; Luzar, A. Electrowetting at the Nanoscale. *J. Phys. Chem. C* **2007**, 505.
(24) Werder, T.; Walther, J. H.; Jaffe, R. L.; Halicioglu, T.; Noca, F.; Koumoutsakos, P. Molecular Dynamics Simulation of Contact Angles of Water Droplets in Carbon Nanotubes. *Nano Lett.* **2001**, 697.
(25) Hirvi, J. T.; Pakkanen, T. A. Molecular Dynamics Simulations of Water Droplets on Polymer Surfaces. *J. Chem. Phys.* **2006**, 144712.
(26) Chen, J.; Chen, W.; Xie, Y.; Wang, Z.; Qin, J. Wettability Behavior of Water Droplet on Organic-Polluted Fused Quartz Surfaces of Pillar-Type Nanostructures Applying Molecular Dynamics Simulation. *Appl. Surf. Sci.* **2017**, *396*, 1058−1066.
(27) Hung, S. W.; Shiomi, J. Dynamic Wetting of Nanodroplets on Smooth and Patterned Graphene-Coated Surface. *J. Phys. Chem. C* **2018**, 8423.
(28) Wang, F.; Wu, H. Molecular Origin of Contact Line Stick-Slip Motion during Droplet Evaporation. *Sci. Rep.* **2015**, *5*, 17521.
(29) Montazeri, K.; Abdolhosseini Qomi, M. J.; Won, Y. Solid-like Behaviors Govern Evaporative Transport in Adsorbed Water Nanofilms. *ACS Appl. Mater. Interfaces* **2020**, 53416.
(30) Solhjoo, S.; Vakis, A. I. Surface Roughness of Gold Substrates at the Nanoscale: An Atomistic Simulation Study. *Tribol. Int.* **2017**, 165.
(31) Liu, H.; Deng, W.; Ding, P.; Zhao, J. Investigation of the Effects of Surface Wettability and Surface Roughness on Nanoscale Boiling Process Using Molecular Dynamics Simulation. *Nucl. Eng. Des.* **2021**, No. 111400.
(32) Liu, H.; Qin, X.; Ahmad, S.; Tong, Q.; Zhao, J. Molecular Dynamics Study about the Effects of Random Surface Roughness on Nanoscale Boiling Process. *Int. J. Heat Mass Transfer* **2019**, No. 118799.
(33) Pham, Q. N.; Zhang, S.; Montazeri, K.; Won, Y. Droplets on Slippery Lubricant-Infused Porous Surfaces: A Macroscale to Nanoscale Perspective. *Langmuir* **2018**, 14439.
(34) McHale, G.; Shirtcliffe, N. J.; Newton, M. I. Contact-Angle Hysteresis on Super-Hydrophobic Surfaces. *Langmuir* **2004**, 10146.
(35) Li, Y.; Diddens, C.; Segers, T.; Wijshoff, H.; Versluis, M.; Lohse, D. Evaporating Droplets on Oil-Wetted Surfaces: Suppression of the Coffee-Stain Effect. *Proc. Natl. Acad. Sci. U. S. A.* **2020**, 16756.
(36) Anantharaju, N.; Panchagnula, M.; Neti, S. Evaporating Drops on Patterned Surfaces: Transition from Pinned to Moving Triple Line. *J. Colloid Interface Sci.* **2009**, 176.
(37) Zuo, Z.; Wang, J.; Huo, Y.; Liu, H.; Xu, R. Particle Motion Induced by Electrostatic Force of a Charged Droplet. *Environ. Eng. Sci.* **2016**, 650.
(38) Vahabi, H.; Wang, W.; Mabry, J. M.; Kota, A. K. Coalescence-Induced Jumping of Droplets on Superomniphobic Surfaces with Macrotexture. *Sci. Adv.* **2018**, No. eaau3488.
(39) Montazeri, K.; Hao, S.; Abdolhosseini Qomi, M. J.; Won, Y. Molecular Dynamics Investigation of Liquid and Vapor Interactions Near an Evaporating Interface: A Theoretical Genetics Perspective. *Adv. Theory Simul.* **2020**, *3*, 2000017.
(40) Bird, J. C.; Dhiman, R.; Kwon, H. M.; Varanasi, K. K. Reducing the contact time of a bouncing drop. *Nature* **2013**, *503*, 385−388.

https://doi.org/10.1021/acs.langmuir.2c03313
Langmuir 2023, 39, 4317−4325

(41) Liu, Y.; Moevius, L.; Xu, X.; Qian, T.; Yeomans, J. M.; Wang, Z. Pancake bouncing on superhydrophobic surfaces. *Nat. Phys.* **2014**, *10*, 515−519.
(42) Gauthier, A.; Symon, S.; Clanet, C.; Quéré, D. Water impacting on superhydrophobic macrotextures. *Nat. Commun.* **2015**, *6*, 8001.
(43) Feng, S.; Zhu, P.; Zheng, H.; Zhan, H.; Chen, C.; Li, J.; Wang, L.; Yao, X.; Liu, Y.; Wang, Z. Three-dimensional capillary ratchet-induced liquid directional steering. *Science* **2021**, *373*, 1344−1348.
(44) Jiang, M.; Wang, Y.; Liu, F.; Du, H.; Li, Y.; Zhang, H.; Toe, S.; Wang, S.; Pan, C.; Yu, J.; Quéré, D.; Whang, Z. Inhibiting the Leidenfrost effect above 1,000 C for sustained thermal cooling. *Nature* **2022**, *601*, 568−572.
(45) Fang, W.; Zhang, K.; Jiang, Q.; Lv, C.; Sun, C.; Li, Q.; Song, Y.; Feng, X. Q. Drop impact dynamics on solid surfaces. *Appl. Phys. Lett.* **2022**, *121*, 210501.
(46) Dalawai, S. P.; Saad Aly, M. A.; Latthe, S. S.; Xing, R.; Sutar, R. S.; Nagappan, S.; Ha, C. S.; Kumar Sadasivuni, K.; Liu, S. Recent Advances in Durability of Superhydrophobic Self-Cleaning Technology: A Critical Review. *Prog. Org. Coat.* **2020**, No. 105381.
(47) Gao, S.; Jiao, L.; Yi, M.; Jin, J.; Wang, X. Mechanism and Research Progress of Anti/de-Icing Using Hydrophobic/Superhydrophobic Surfaces. *Acta Aerodyn. Sin.* **2021**, DOI: 10.7638/kqdlxxb-2020.0179.
(48) Boreyko, J. B.; Srijanto, B. R.; Nguyen, T. D.; Vega, C.; Fuentes-Cabrera, M.; Collier, C. P. Dynamic Defrosting on Nanostructured Superhydrophobic Surfaces. *Langmuir* **2013**, 9516.
(49) Plimpton, S. Fast parallel algorithms for short-range molecular dynamics. *J. Comput. Phys.* **1995**, *117*, 1−19.
(50) Abascal, J. L. F.; Vega, C. A general purpose model for the condensed phases of water: TIP4P/2005. *J. Chem. Phys.* **2005**, *123*, 234505.
(51) Hockney, R. W., Eastwood, J. W., 2021. *Computer simulation using particles*. Crc Press, DOI: 10.1201/9780367806934.

https://doi.org/10.1021/acs.langmuir.2c03313
Langmuir 2023, 39, 4317−4325